From Design Complexity to Build Quality in Additive Manufacturing—A Sensor-Based Perspective

Ruimin Chen^{1 (1)}, Farhad Imani^{1 (1)}, Edward Reutzel², and Hui Yang^{1,* (1)}

Manuscript received September 14, 2018; revised October 11, 2018; accepted October 31, 2018. Date of publication November 12, 2018; date of current version January 16, 2019.

Abstract—Additive manufacturing (AM) provides a greater level of flexibility to build parts with complex structures than the traditional subtractive manufacturing. However, the more complex the engineering design is, the greater challenge is posed on the AM machine. To cope with such complexity, advanced imaging is increasingly invested to increase the information visibility. There is an urgent need to leverage the available imaging data to investigate the interrelationships between design complexity and quality characteristics of AM builds. This article presents a design of experiments on the laser powder bed fusion machine to investigate how design parameters (i.e., recoating orientation, hatching pattern, width, and height) influence edge roughness in thin-wall structures of the final builds. First, we perform the postbuild inspection of final builds and collect large amounts of X-ray computed tomography (XCT) images. Second, we integrate the computer-aided designs with XCT images for image registration and then characterize the edge roughness of each layer in a thin wall of the AM build. Finally, we perform an analysis of variance with respect to design parameters and develop a regression model to predict how build design impacts the edge roughness in each layer of the thin-wall structures. Experimental results show that edge roughness is sensitive to recoating orientations, width, and hatching patterns. This article sheds insights on the optimization of engineering design to improve the quality of AM builds.

Index Terms—Sensor data fusion, additive manufacturing (AM), data fusion model, design of experiments, sensor-based design.

I. INTRODUCTION

Additive manufacturing (AM) provides a greater level of flexibility to build parts with complex structures than the traditional subtractive manufacturing [1]. This revolutionary technology also results in the shorter lead time and the ability to produce parts directly from computer-aided designs (CAD) without the need for expensive partspecific tooling [2]. However, AM nowadays is still limited in the ability to achieve the high level of quality and repeatability, thereby hampering the widespread application of the technology in the manufacturing industry. In the AM process, there are a number of factors impacting the quality of final builds, such as powder materials, chamber environment, machine and process settings, and design complexity. Our prior studies focused on the effects of machine and process settings (e.g., laser power, scanning velocity, and hatch spacing) on the quality of final builds [3], [4]. In addition, we characterized the multifractal patterns of in situ layerwise images for the estimation of defect states in each layer [5], [6] and then developed a Markov decision process model to sequentially optimize the quality of AM builds [7]. As a further step, we focus on the interrelationships between design complexity and quality characteristics of AM builds.

It is well known that the design complexity poses significant challenges on traditional subtractive manufacturing. AM provides more design freedom, and complex structures can now be fabricated layer-by-layer with the new AM technology. However, a higher level of design complexity can greatly degrade the quality of final AM builds. Advanced imaging is increasingly utilized to increase the visibility of

Corresponding author: Hui Yang (e-mail: huy25@psu.edu). Associate Editor: X. Jin. Digital Object Identifier 10.1109/LSENS.2018.2880747

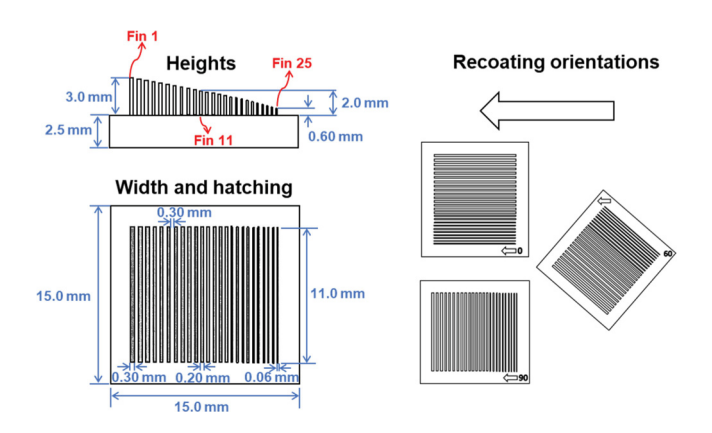


Fig. 1. Front and top views of CAD model and recoating orientations.

postbuild quality information in the face of increasing design complexity. Realizing the full potential of readily available imaging data calls upon the investigation of the interrelationships between design complexity and quality characteristics of AM builds. Therefore, this article presents our experimental studies on the laser powder bed fusion (LPBF) machine to investigate how design parameters (i.e., recoating orientation, hatching pattern, width, and height) influence edge roughness in thin-wall structures of the final builds.

As shown in Fig. 1, our experiments feature a thin-wall structure with different recoating orientations, widths, heights, and hatching patterns (see Section II-A). Thin-wall structures are widely used in heat exchanger designs. A total of three thin-wall parts (also called fin parts) were built, each differing in the manner of rotation upon the

¹Department of Industrial and Manufacturing Engineering,The Pennsylvania State University, University Park, PA 16802 USA

²Applied Research Laboratory, The Pennsylvania State University, State College PA 16802 USA

^{*}Senior Member, IEEE

Fig. 2. Flow diagram of the proposed research methodology.

build plate, i.e., their planar inclination in the *X*–*Y* plane with respect to the recoater blade travel within the machine. After fabrication, we performed postbuild inspection with the X-ray computed tomography (XCT). Next, the XCT images were registered layer-by-layer with the original CAD files to extract the quality features of edge roughness in each thin wall. Here, the edge roughness refers to the geometric deviation of build in the registered XCT scan and CAD file. However, the average of absolute values of the profile height deviations from the mean line is generally used for edge characterization. These features were tracked across layers to detect impending collapse of thin-wall failures. Finally, we performed an analysis of variance with respect to design parameters and further developed a regression model to predict how design complexity impacts the edge roughness in each layer of the thin-wall structures.

II. RESEARCH METHODOLOGY

As shown in Fig. 2, the present investigation focuses on metal printing with the EOS M280 LPBF machine. The data utilized in this study consist of the CAD design files (i.e., the expected quality) and the XCT images of each layer in the thin wall (i.e., the delivered quality).

A. Experimental Setup and Factors

In this experiment, raw materials are Spherical ASTM B348 Grade 23 Ti-6Al-4V powder, available from the LPW technology, with a size distribution of 14–45 μ m. Each fin part comprises a 15 mm \times 15 mm \times 55 mm platform upon which are built a total of 25 fin walls. The experimental factors, such as orientation, width, height, and hatching pattern are detailed as follows.

- Orientation: Fin parts were built vertically upward with layer thickness of 60 μm in three orientations with respect to the recoater blade travel direction (i.e., 0°, 60°, and 90°). The arrow (see Fig. 1) shows the recoating direction.
- Width: The width of fin walls varies from 0.06 to 0.3 mm with the step size of 0.01 mm and the distance between two fins is 0.3 mm.
- 3) *Height:* The designed height of fin walls differs from 0.6 to 3.0 mm with the step size of 0.1 mm. Note that the height is proportional to the width in each thin wall with an aspect ratio of 0.1 (see Fig. 1).

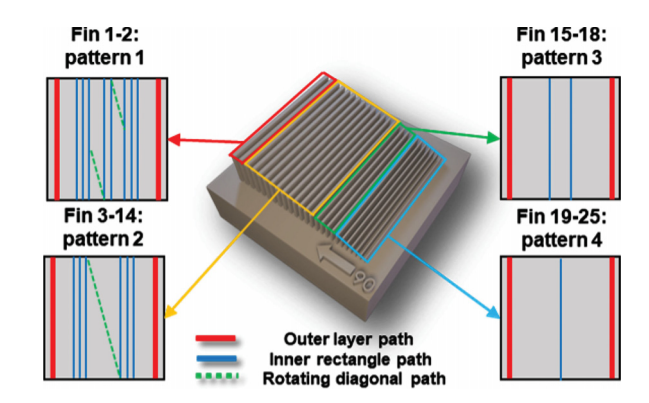


Fig. 3. Hatching patterns of the fin walls.

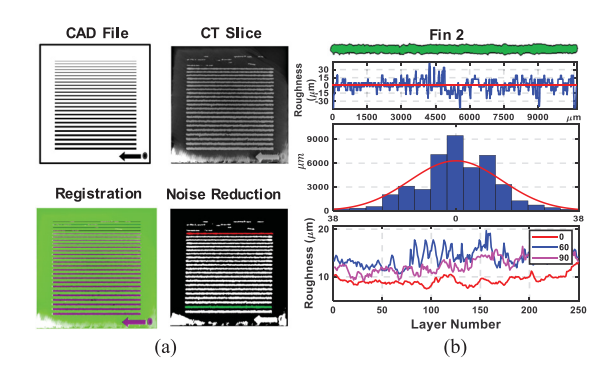


Fig. 4. (a) Image registration and edge extraction of fin walls. (b) Normality assumption and verification through layer of fin 2 (unit: μ m).

4) *Hatching:* The four hatching patterns of fin walls, which employ the standard EOS processing path, are significantly different as the width increases (see the design in Fig. 3).

B. Image Registration and Edge Characterization

This experiment uses postbuild X-ray CT images to quantify the geometric variations of each fin. Although metrology methods, such as 3-D scanning or coordinate measuring machines, are widely used to measure the geometric dimensionality, they are limited in the resolution to comprehensively measure the 3-D geometry of fin builds. High-end X-Ray CT, albeit expensive, offers an advantage to examine the internal structure of the builds, as well as quantify the 3-D geometric variations of the build.

For each fin part, we have a CAD file and the corresponding post-build XCT data. Note that we slice the 3-D CAD model and XCT volumetric scans into 300 layers (i.e., with a thickness of $10~\mu m$ per layer). To transform the two sources of data into a single coordinate system, we perform a shape-to-image intensity-based registration and extract the region of interests. Intensity-based methods consider correlation metrics to compare the intensity patterns in the target image (i.e., XCT) and the source image (i.e., CAD). The registration process aims to transform (i.e., affine transformation) the target image into the source image. After registration, we remove noise (i.e., connected objects that are less than 20 pixels) and extract fin walls for each layer.

As illustrated in Fig. 4(a), by defining the edge from the CAD file as the referencing horizontal axis, we first measure the distance between the edge of the registered XCT scan and the CAD file and then concatenate the upper and lower edge signals to generate the edge roughness signal [see top right of Fig. 4(b)]. Fig. 4(b) shows that the signal is approximately represented by a normal distribution for

				F		
		Fin 1	Fin 2		Fin 20	Fin 21
0	0°	$\sigma_1, \sigma_2,, \sigma_{299}, \sigma_{300}$	$\sigma_1, \sigma_2,, \sigma_{289}, \sigma_{290}$		$\sigma_1, \sigma_2,, \\ \sigma_{109}, \sigma_{110}$	
	60°	$\sigma_1, \sigma_2,, \sigma_{299}, \sigma_{300}$	$\sigma_1, \sigma_2,, \sigma_{289}, \sigma_{290}$		$\sigma_1, \sigma_2,, \\ \sigma_{109}, \sigma_{110}$	
	90°	$\sigma_1, \sigma_2,, \sigma_{299}, \sigma_{300}$	$\sigma_1, \sigma_2,, \sigma_{289}, \sigma_{290}$		$\sigma_1, \sigma_2,, \\ \sigma_{109}, \sigma_{110}$	

Fig. 5. Experimental data structure for the ANOVA analysis: ${\it F}$ and ${\it O}$ represent two factors, namely fin number and orientation.

the fin 2 of layer 11. It is worth mentioning that the characteristics of edge roughness of fin wall 2 are different under the changing recoating directions (see bottom right of Fig. 4). After approximating the edge signals with a normal distribution, we obtained the standard deviation (STD) of each edge in each layer of a thin wall for further analysis.

C. Analysis of Variance

Here, we perform the two way analysis of variance (ANOVA) to study the effects of experimental factors, i.e., orientations and fin wall characteristics, on the part quality. Note that the parameters of height, width, and hatching pattern are affiliated with the fin wall number in our design of experiments. Therefore, we rearrange four parameters into two factors (i.e., orientation and fin wall characteristics).

As shown in Fig. 5, there are three levels of orientation with respect to the recoater blade travel direction and 21 levels of thin wall. It is worth mentioning that the last four fin walls were collapsed in the fabrication process, likely due to interference with the recoater blade during recoat operations, and therefore, they are not available for ANOVA. Here, fin 1 to fin 21 are taken into account for this ANOVA analysis. The model is expressed as follows:

$$\sigma_{ij} = \beta_0 + \beta_1 \times O_i + \beta_2 \times F_j + \beta_3 \times O_i \times F_j + \varepsilon_{ij}$$
 (1)

where O and F represent the orientation and the fin number, respectively. Also, ε_{ij} in (1) denotes the error term in ANOVA model.

D. Predictive Modeling

In addition, we develop a regression model to quantify the relationship between edge roughness and the orientation, width, height, and hatching pattern of each fin wall

$$\sigma = \beta_0 + \beta_1 \times O + \beta_2 \times W + \beta_3 \times H + \beta_4 \times Ha + \beta_5 \times O \times W$$
$$+ \beta_6 \times O \times H + \beta_7 \times O \times Ha + \beta_8 \times W \times H + \beta_9 \times W \times Ha$$
$$+ \beta_{10} \times H \times Ha + \varepsilon \tag{2}$$

where Ha denotes the hatching pattern and is a categorical variable with four levels, O stands for the orientation, which is also a categorical variable with three levels, and H and W represents the height and width of the corresponding fin wall, respectively. The R-square (R^2) is utilized to statistically measure the performance of the model, and is defined as $R^2 = 1 - \frac{\text{Sum of Square}_{\text{residual}}}{\text{Sum of Square}_{\text{total}}} = 1 - \frac{\sum_i (\sigma_i - \hat{\sigma}_i)^2}{\sum_i (\sigma_i - \hat{\sigma}_i)^2}$. Where (σ_i) is the edge roughness, $(\hat{\sigma_i})$ is the predicted value of the variance, and $(\overline{\sigma})$ is the overall average of the data.

Table 1. ANOVA analysis of variance in two-way layout experiment.

Source	Sum Sq.	d.f.	Mean Sq.	F	Prob>F
fin	200.472	20	10.024	20.412	0
orientation	631.408	2	315.704	642.890	0
fin * orientation	307.300	40	7.683	15.644	0
Error	6156.050	12536	0.491		
Total	7371.040	12598			

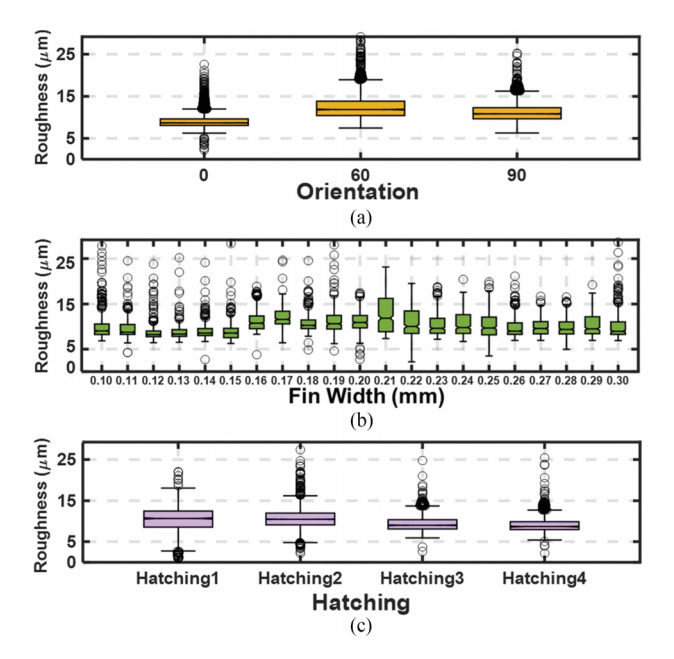


Fig. 6. (a) Mean and STD of edge roughness under three orientations. (b) Mean and STD of edge roughness when fin width increases. (c) Mean and STD of edge roughness for hatching patterns.

III. EXPERIMENTAL RESULTS

A. Statistical Analysis

1) Analysis of Variance to Test the Hypothesis Whether Orientations and Fin Wall Characteristics Impact the Edge Roughness: In Table 1, the *p*-values for orientation, fin wall, and interaction are approximately 0, which shows all the three factors have significant impacts on the edge roughness. In this ANOVA table, the Sum Sq., d.f., mean Sq., *F*, and Prob>*F* denote sum of squared errors, degrees of freedom, mean of squared errors, the *F* statistics, and the *p*-value, respectively.

- 2) Impact of Orientation on Edge Characteristics: As shown in Fig. 6(a), the average variation of fin wall edges is not constant for different recoating directions. Note that building the fin part at 0° orientation with respect to recoating direction leads to the smallest edge roughness, whereas the biggest edge roughness occurs at 60° .
- 3) Impact of Fin Width on Edge Characteristics: As illustrated in Fig. 6(b), the mean of edge roughness first increases and then decreases as the fin wall gets wider. The variations of edge roughness is bigger when the fin width is smaller. Fig. 6(b) shows that as the width of fin walls increases, the AM machine can print the thin-wall structure with smaller variations of edge roughness. When the width is as small as 0.10–0.19 mm, there are more outliers indicating that significant variations in surface roughness can occur when building thin-wall structures.
- 4) Impact of Hatching Pattern on Edge Characteristics: As shown in Fig. 6(c), hatching patterns 1 and 2 have similar impacts on the edge quality, but hatching patterns 3 and 4 yield smaller mean in the edge

Table 2. Results of regression analysis.

Effect	Estimate	Error	t value	P value
Intercept	-5.844	2.327	-2.522	0.016
hatching 2	7.554	2.316	3.262	0.002
hatching 3	7.096	2.339	3.034	0.004
hatching 4	8.496	2.374	3.579	0.001
width	24.138	7.853	3.074	0.004
orientation 60	0.026	0.133	1.974	0.055
orientation 90	-0.177	0.299	-0.592	0.557
width * orientation 60	-0.188	0.968	-0.195	0.847
width * orientation 90	2.249	0.979	2.298	0.027
hatching 2 * orientation 60	0.466	0.139	3.359	0.002
hatching 3 * orientation 60	0.132	0.101	1.310	0.198
hatching 4 * orientation 60	NA	NA	NA	NA
hatching 2 * orientation 90	-0.160	0.108	-1.490	0.145
hatching 3 * orientation 90	-0.206	0.182	-1.137	0.263
hatching 4 * orientation 90	-0.243	0.208	-1.167	0.251
hatching 2 * width	-26.093	7.853	-3.323	0.002
hatching 3 * width	-24.627	8.176	-3.012	0.005
hatching 4 * width	-35.818	9.069	-3.950	0.003

roughness. It is also worth noting that the spread of the edge roughness decreases with hatching patterns 3 and 4.

B. Predictive Modeling

Next, we develop a regression model to quantify the relationship between the edge roughness and design parameters. As shown in Table 2, hatching patterns, width, and two-way interactions of width × orientation, hatching × orientation, and hatching × width are significant at the confidence level of 95%. It can be seen that the p-value of hatching pattern 4 is the lowest compared with the p-values of the other hatching patterns. Hatching pattern 4 is the simplest one and has the most accentuated impact on the edge roughness. Switching from the other patterns may not change the edge roughness as much as pattern 4. Note that the pattern is determined by software based on the designed width. For further investigation, hatching patterns can be adjusted to generate fins with reduced edge roughness, even for thin fins. Besides, the p-value of width is 0.039, which shows that it is an important factor in edge roughness. Also, two-way interaction terms of hatching \times orientation and width \times orientation are significant, which shows that the combination of different design parameters impacts the quality in AM as well. Here, we set the hatching pattern 1 and the 0° orientation as the baseline, and the NA indicates that the variable is correlated with one of the other variables.

The coefficient of determination is utilized to illustrate the percentage of variation in response variable that is explained by the model. The regression model yields the R-squared statistic of 94.79% and adjusted R-squared statistic of 92.54%, showing that variations in response variable are highly dependent on design parameters. Further, we utilize the plot of residual versus fitted value and normal Q-Q plot as descriptive graphical tools for the model diagnosis and checking the normality assumption of residuals. Fig. 7(a) shows that the plot of residual versus fitted value does not show a systematic pattern, and Fig. 7(b) shows the normal Q–Q plot approximately follows a straight line.

IV. CONCLUSION

AM provides the design freedom with complex geometrical structures, which cannot be realized otherwise using conventional manu-

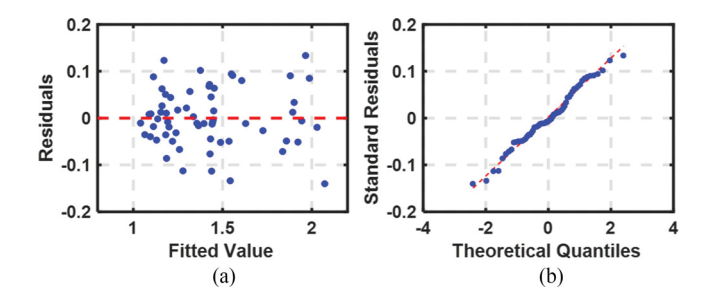


Fig. 7. (a) Residual versus fitted value of the regression model. (b) Normal Q-Q plot of the regression model.

facturing methods. However, a higher level of design complexity can significantly deteriorate the quality of AM builds. To tackle this challenge, postbuild high-resolution XCT scans that provide a rich data environment are recently taken into account. There is a dire need to take advantage of this data to decipher the relationship between design parameters and quality of AM builds. In this study, a design of experiments is performed to characterize the impact of design parameters on edge roughness of thin-wall structures. First, XCT images of builds are registered to CAD models to characterize and quantify the edge roughness in thin-wall structures. Then, we performed the experimental design to study the impact of design parameters on the edge quality of fins. Next, a predictive model is developed to quantify the behavior of edge roughness as a function of these parameters. The regression result shows that the hatching, width, and orientation have significant impacts on the edge roughness at the confidence level of 95%. Furthermore, the adjusted R-squared demonstrates that 92.54% of the edge roughness can be explained by the regression model. This study sheds insights to optimize the engineering design for quality improvement in AM.

ACKNOWLEDGMENT

This work was supported in part by the NSF Center for e-Design (Lockheed Martin) and in part by the NSF CAREER Grant (CMMI-1617148). The authors gratefully acknowledge the valuable contributions and suggestions from the Center for Innovative Material Processing Through Direct Digital Deposition at Penn State, especially C. Dickman, G. Gundermann, M. Dolack, Dr. T. Simpson, and Dr. A. Nassar, for this research.

REFERENCES

- [1] J. Boyer, C. Seepersad, T. W. Simpson, C. B. Williams, and P. Witherell, "Special section: Designing for additive manufacturing recent advances in design for additive manufacturing," ASME J. Mech. Des., vol. 139, no. 10, 2017, Art. no. 100901.
- [2] E. W. Reutzel and A. R. Nassar, "A survey of sensing and control systems for machine and process monitoring of directed-energy, metal-based additive manufacturing, Rapid Prototyping J., vol. 21, no. 2, pp. 159-167, 2015.
- [3] F. Imani, A. Gaikwad, M. Montazeri, P. Rao, H. Yang, and E. Reutzel, "Process mapping and in-process monitoring of porosity in laser powder bed fusion using layerwise optical imaging," J. Manuf. Sci. Eng., vol. 140, no. 10, 2018, Art. no. 101009.
- [4] F. Imani, A. Gaikwad, M. Montazeri, H. Yang, and P. Rao, "Layerwise in-process quality monitoring in laser powder bed fusion," in Proc. ASME 13th Int. Manuf. Sci. Eng. Conf., 2018, paper no. MSEC2018-6477.
- [5] F. Imani, B. Yao, R. Chen, P. Rao, and H. Yang, "Fractal pattern recognition of image profiles for manufacturing process monitoring and control," in Proc. ASME 13th Int. Manuf. Sci. Eng. Conf., 2018, paper no. MSEC2018-6523.
- [6] B. Yao, F. Imani, A. S. Sakpal, E. Reutzel, and H. Yang, "Multifractal analysis of image profiles for the characterization and detection of defects in additive manufacturing," J. Manuf. Sci. Eng., vol. 140, no. 3, 2018, Art, no. 031014.
- [7] B. Yao, F. Imani, and H. Yang, "Markov decision process for image-guided additive manufacturing," IEEE Robot, Automat, Lett., vol. 3, no. 4, pp. 2792–2798, Oct. 2018.